Science and Technology Publishing (SCI & TECH)
ISSN: 2632-1017
Vol. 3 Issue 10, October - 2019

Analysis Of Antenna Point Loss In Satellite Communication Link

Dike Happiness Ugochi[1]
Department of Electrical/Electronic Engineering, Imo State University (IMSU),
Owerri, Imo State , Nigeria
Corresponding Author: happiness@siat.ac.cn

Isaac A. Ezenugu[2]
Department of Electrical/Electronic Engineering, Imo State University (IMSU),
Owerri, Imo State , Nigeria
isaac.ezenugu@yahoo.com

Abstract— **In this paper, analysis of antenna point loss in satellite communication link is presented. Basically, the antenna misalignment (de-pointing) loss is a function of the pointing error and the 3 dB beamwidth of the antenna. Particularly, the paper focuses on the variation of the antenna pointing loss on frequency and on the antenna diameter. The analysis was for a parabolic antenna. Frequencies between 2 GHz and 40 GHz and antenna pointing error between 0 ° and 1° were considered in the numerical computations. The results show that for antenna operating at frequency, f of 6 GHz and diameter, d of 3 m, the antenna pointing loss was 0.088163 dB at 0.1° pointing error and 8.816327 dB at 1° pointing error. Also, the results for the antenna pointing loss (Lp in dB) at 2 GHz, 6 GHz, 12 GHz , 20 GHz, and 40 GHz for 0° ≤ θ_T ≤ 1° and d of 3 m showed that the antenna pointing loss (Lp in dB) increases with pointing error angle (θ). Also, for a given pointing error angle (θ) and antenna diameter d (in m) the antenna pointing loss (Lp in dB) increases with frequency, f. Also, the results for the computation of antenna pointing loss at diameter, d of 0.5 m, 1 m, 2 m , 4 m, and 8 m for 0° ≤ θ_T ≤ 1° and frequency, f of 12 GHz show that for a given frequency and pointing error angle (θ), the antenna pointing loss (Lp in dB) increases with antenna diameter (d). In essence, satellite link designers should ensure minimal pointing error especially for the higher frequencies and for large antenna sizes.**

Keywords— Antenna, satellite link, pointing error, beam width, 3dB beam width, antenna pointing loss

1. INTRODUCTION

Over the years, satellite communications have grown to become the foremost technologies for global telecommunication [1,2,3,4]. Increasingly, more users and divers applications are supported by satellite communication systems [5,6,7,8]. This places more demand on bandwidth and quality of service requirements. As such, satellite link designers are facing increasingly challenges to design high efficient satellite communication links that meet the stringent quality of service using cost effective technologies [9,10,11,12,13].

Among other things, antenna pointing or misalignment loss is one of the losses that are considered in satellite link design [14,15,16,17,18,19]. The two notable antenna misalignment losses are the off-axis loss at the satellite and the off-axis loss at the ground station [20]. The off-axis loss at the satellite is addressed during the link design by ensuring that the antenna is pointed appropriately within the satellite antenna contour. The antenna pointing loss at the earth station is determined using some analytical and statistical approaches.

Basically, antenna misalignment or pointing loss is the reduction in signal strength due to the antenna pointing error or antenna misalignment. Studies have shown that the antenna pointing loss is a function of certain parameters among which are antenna beamwidth, antenna size and antenna misalignment error [21,22,23,24]. Accordingly, in this paper, the focus is on the variation of the antenna pointing loss on frequency, misalignment error and on the antenna diameter. Numerical examples are used to evaluate the variation of the antenna pointing loss among different microwave frequency ranges. Relevant analytical expressions for the computations are presented. The ideas presented in this paper are useful for satellite link budget analysis, especially in the microwave frequency range.

2.1 METHODOLOGY

The antenna misalignment (de-pointing) loss is a function of the pointing error and the 3 dB beamwidth of the antenna. The image of the 3 dB (θ_{3dB}) beam width (in degrees) for parabolic antenna is shown in Figure 1. The 3 dB (θ_{3dB}) beamwidth (in degrees) for parabolic antenna is given in terms of the antenna dish diameter, d (in m) and wavelength , ʎ (in m) and it is given as follows;

$$\theta_{3dB} = \frac{70(ʎ)}{d} \quad (1)$$

where

$$ʎ = \frac{3x10^8}{f} \quad (2)$$

$$\theta_{3dB} = \frac{70}{d}\left(\frac{3x10^8}{f}\right) \quad (3)$$

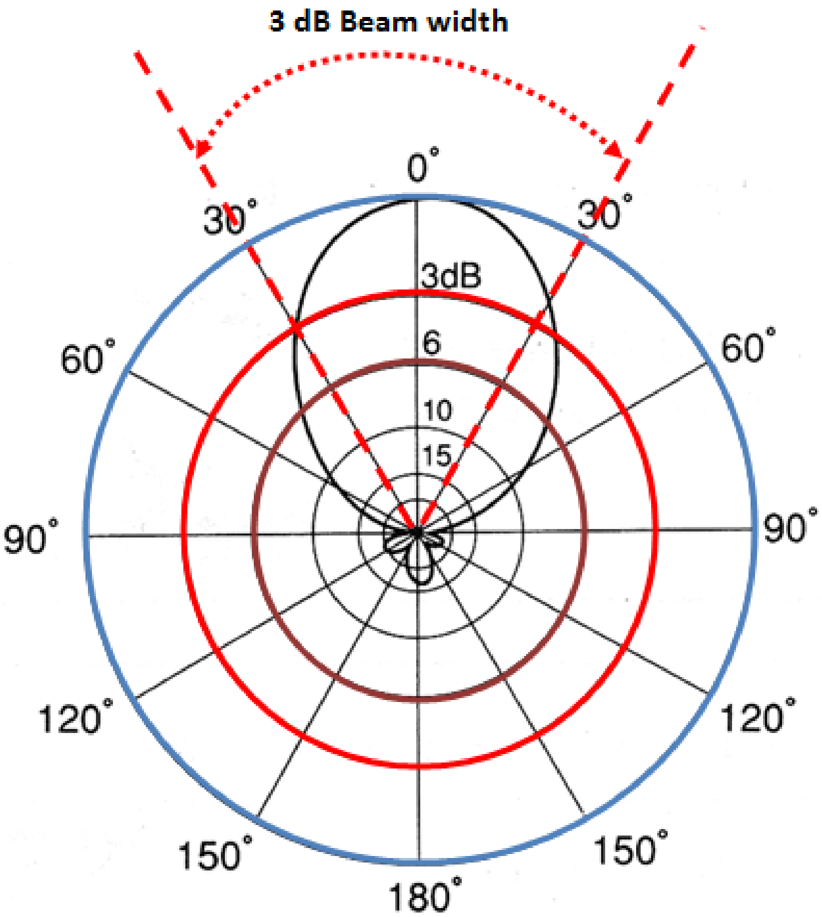

Figure 1 The image of the 3 dB (θ_{3dB}) beam width (in degrees) for parabolic antenna

The antenna transmitter pointing error, θ_T and the receiver antenna pointing error, θ_R (as shown in Figure 2) are used to determine the antenna pointing losses at the transmitter , $L_{\theta T}$ and at the receiver, $L_{\theta R}$ as follows;

$$L_{\theta T} = 12\left(\frac{\theta_R}{\theta_{T3dB}}\right)^2 \quad (4)$$

$$L_{\theta R} = 12\left(\frac{\theta_R}{\theta_{R3dB}}\right)^2 \quad (5)$$

The expressions for $L_{\theta T}$ and $L_{\theta R}$ are valid for $\theta_T \leq 1°$ and $\theta_R \leq 1°$ respectively. In terms of antenna diameter, d, the wavelength, λ and frequency, f, the antenna pointing losses of the transmitter antenna is given as;

$$L_{\theta T} = 12\left(\frac{\theta_T}{\theta_{T3dB}}\right)^2 = 12\left(\frac{\theta_T}{\frac{70(\lambda)}{d_T}}\right)^2 = 12\left(\frac{\theta_R(d_T)}{70(\lambda)}\right)^2 \quad (6)$$

$$L_{\theta T} = 12\left(\frac{\theta_R(d_T)}{70}(\frac{1}{\lambda})\right)^2 = 12\left(\frac{\theta_R(d_T)}{70}(\frac{f}{3x10^8})\right)^2 \quad (7)$$

Similarly, for the receiver antenna, the point loss is given as;

$$L_{\theta R} = 12\left(\frac{\theta_R}{\theta_{R3dB}}\right)^2 \quad (8)$$

$$L_{\theta T} = 12\left(\frac{\theta_R}{\theta_{R3dB}}\right)^2 = 12\left(\frac{\theta_R(d_R)}{70}(\frac{1}{\lambda})\right)^2 \quad (9)$$

$$L_{\theta T} = 12\left(\frac{\theta_R(d_R)}{70}(\frac{f}{3x10^8})\right)^2 \quad (10)$$

The antenna pointing error loss is computed for various frequencies and also for various antenna diameters. The computation is conducted for $0° \leq \theta_T \leq 1°$.

3. RESULTS AND DISCUSSION

The detailed results for the computation of antenna pointing loss at 6 GHz for $0° \leq \theta_T \leq 1°$ and d = 3 m are given in Table 1. Also, the results for the computation of antenna pointing loss at 2 GHz, 6 GHz, 12 GHz , 20 GHz, and 40GHz for $0° \leq \theta_T \leq 1°$ and d = 3 m are given in Table 2. The graph plot for antenna pointing loss at 2 GHz and 6 GHz, for $0° \leq \theta_T \leq 1°$ and d = 3 m is given in Figure 2 while graph plot for antenna pointing loss at 12 GHz , 20 GHz and 40 GHz, for $0° \leq \theta_T \leq 1°$ and d = 3 is given in Figure 3. According to the results, for a given frequency and antenna diameter, the antenna pointing loss (Lp in dB) increases with pointing error angle (θ). Also, for a given pointing error angle (θ) and antenna diameter (d in m) the antenna pointing loss (Lp in dB) increases with frequency ,f.

Table 1 The detailed results for the computation of antenna pointing loss (Lp in dB) at 6 GHz for $0° \leq \theta_T \leq 1°$ and d = 3 m

f (GHZ)	ʎ (m)	D (m)	Antenna 3 dB Beamwidth (θ3dB °)	Pointing Error Angle (θ°)	LP for 6 GHz **(Lp in dB)**
6	0.05	3	1.166667	0	0
6	0.05	3	1.166667	0.1	0.088163
6	0.05	3	1.166667	0.2	0.352653
6	0.05	3	1.166667	0.3	0.793469
6	0.05	3	1.166667	0.4	1.410612
6	0.05	3	1.166667	0.5	2.204082
6	0.05	3	1.166667	0.6	3.173878
6	0.05	3	1.166667	0.7	4.32
6	0.05	3	1.166667	0.8	5.642449
6	0.05	3	1.166667	0.9	7.141224
6	0.05	3	1.166667	1	8.816327

Table 2 The results for the computation of antenna pointing loss (Lp in dB) at 2 GHz, 6 GHz, 12 GHz , 20 GHz, and 40GHz for $0° \leq \theta_T \leq 1°$ and d = 3 m

Pointing Error Angle (θ°)	LP for 2 GHz **(Lp in dB)**	LP for 6 GHz **(Lp in dB)**	LP for 12GHz **(Lp in dB)**	LP for 20 GHz **(Lp in dB)**	LP for 40 GHz **(Lp in dB)**
0	0	0	0	0	0
0.1	0.009796	0.088163	0.352653	0.979592	3.918367
0.2	0.039184	0.352653	1.410612	3.918367	15.67347
0.3	0.088163	0.793469	3.173878	8.816327	35.26531
0.4	0.156735	1.410612	5.642449	15.67347	62.69388
0.5	0.244898	2.204082	8.816327	24.4898	97.95918
0.6	0.352653	3.173878	12.69551	35.26531	141.0612
0.7	0.48	4.32	17.28	48	192
0.8	0.626939	5.642449	22.5698	62.69388	250.7755
0.9	0.793469	7.141224	28.5649	79.34694	317.3878
1	0.979592	8.816327	35.26531	97.95918	391.8367

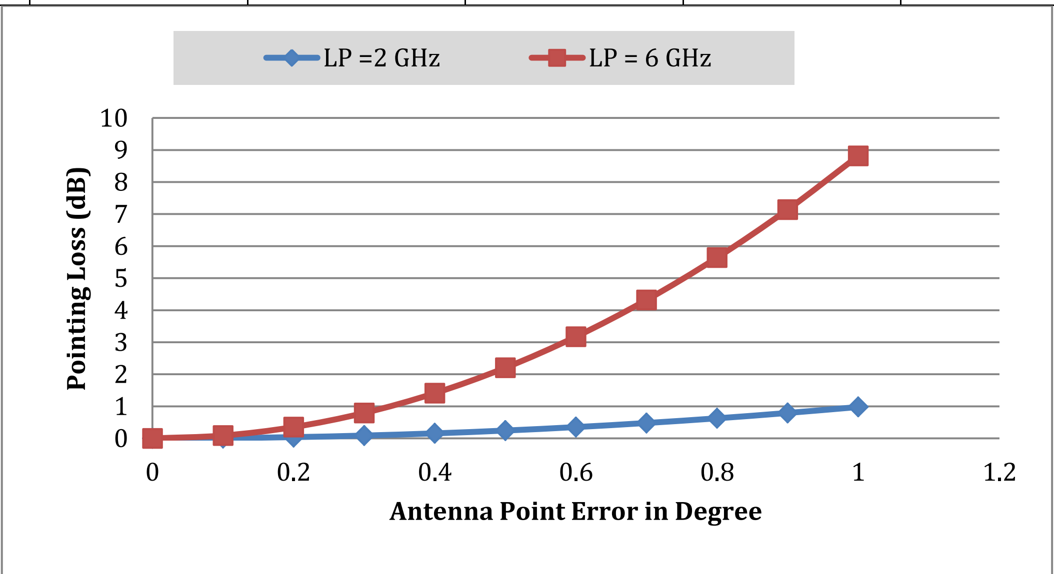

Figure 2 The antenna pointing loss at 2 GHz and 6 GHz, for $0° \leq \theta_T \leq 1°$ and d = 3 m

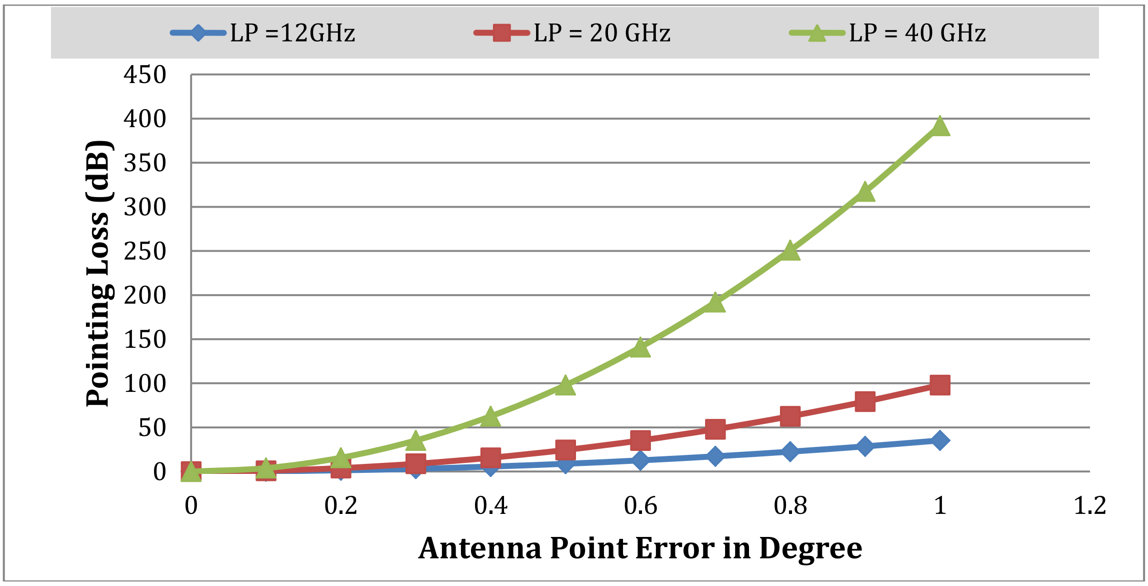

Figure 3 The antenna pointing loss at 12 GHz , 20 GHz and 40 GHz, for 0° ≤ θ_T ≤ 1° and d = 3 m

The detailed results for the computation of antenna pointing loss at 6 GHz for 0° ≤ θ_T ≤ 1° and d = 6 m are given in Table 3. Also, the results for the computation of antenna pointing loss at d =0.5 m, d = 1 m, d = 2 m z , d = 4 m, and d = 8 m for 0° ≤ θ_T ≤ 1° and f = 12 GHz are given in Table 4. The graph plot for antenna pointing loss at d = 0.5 m and d = 1 m, for 0° ≤ θ_T ≤ 1° and f = 12 GHz m is given in Figure 4 while graph plot for antenna pointing loss at d = 2 m z , d = 4 m, and d = 8 m for 0° ≤ θ_T ≤ 1° and f = 12 GHz is given in Figure 5. According to the results, for a given frequency and pointing error angle (θ), the antenna pointing loss (Lp in dB) increases with antenna diameter (d).

Table 3. The detailed results for the computation of antenna pointing loss at 6 GHz for 0° ≤ θ_T ≤ 1° and d = 6 m

f (GHZ)	ʎ (m)	d	θ3dB	θ	Lp (dB) for 6 GHz
6	0.05	6	0.583333	0	0
6	0.05	6	0.583333	0.1	0.352653
6	0.05	6	0.583333	0.2	1.410612
6	0.05	6	0.583333	0.3	3.173878
6	0.05	6	0.583333	0.4	5.642449
6	0.05	6	0.583333	0.5	8.816327
6	0.05	6	0.583333	0.6	12.69551
6	0.05	6	0.583333	0.7	17.28
6	0.05	6	0.583333	0.8	22.5698
6	0.05	6	0.583333	0.9	28.5649
6	0.05	6	0.583333	1	35.26531

Table 4 The results for the computation of antenna pointing loss at d =0.5 m, d = 1 m, d = 2 m z , d = 4 m, and d = 8 m for 0° ≤ θ_T ≤ 1° and f = 12 GHz

θ°	Lp (dB) for d =0.5 m	Lp (dB) for d =1m	Lp (dB) for d =2 m	Lp (dB) for d =4m	Lp (dB) for d =8 m
0	0	0	0	0	0
0.1	0.009796	0.039184	0.156735	0.626939	2.507755
0.2	0.039184	0.156735	0.626939	2.507755	10.03102
0.3	0.088163	0.352653	1.410612	5.642449	22.5698
0.4	0.156735	0.626939	2.507755	10.03102	40.12408
0.5	0.244898	0.979592	3.918367	15.67347	62.69388
0.6	0.352653	1.410612	5.642449	22.5698	90.27918
0.7	0.48	1.92	7.68	30.72	122.88
0.8	0.626939	2.507755	10.03102	40.12408	160.4963
0.9	0.793469	3.173878	12.69551	50.78204	203.1282
1	0.979592	3.918367	15.67347	62.69388	250.7755

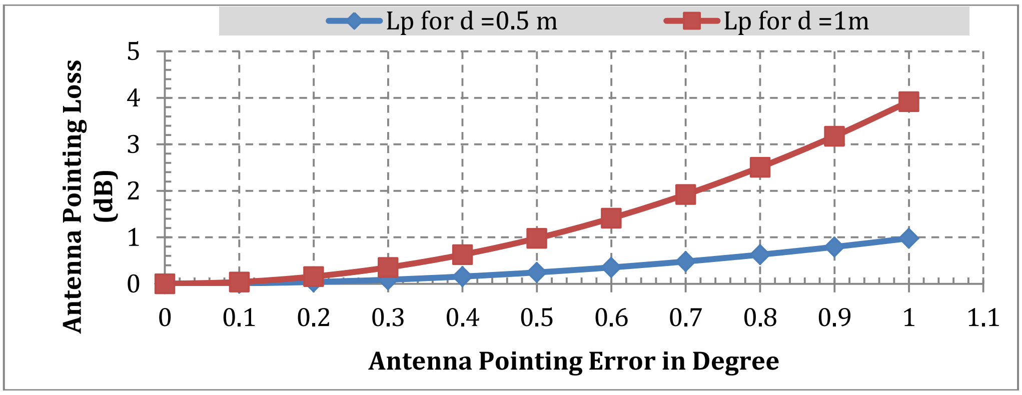

Figure 4 The graph plot for antenna pointing loss at d = 0.5 m and d = 1 m, for $0° \leq \theta_T \leq 1°$ and f = 12 GHz m

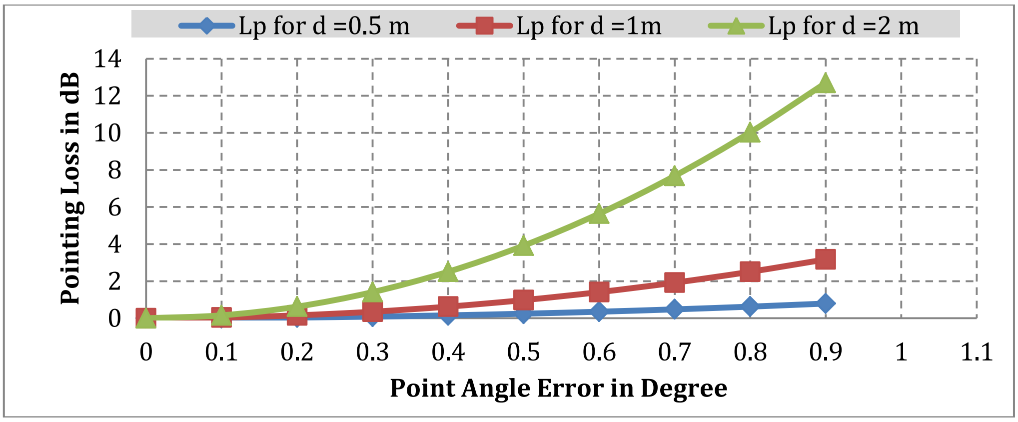

Figure 5. The graph plot for antenna pointing loss at d = 2 m z , d = 4 m, and d = 8 m for $0° \leq \theta_T \leq 1°$ and f = 12 GHz

4. CONCLUSION

The computation of antenna pointing loss for satellite link is presented. The paper focuses on the variation of the antenna pointing loss on frequency and on the antenna diameter. The results show that the bigger the antenna diameter, the more the effect of antenna pointing error will be . Also, for a given antenna diameter, higher frequencies have higher antenna pointing loss for any given pointing alignment error. Essentially, satellite link designers should ensure minimal pointing error especially for the higher frequencies and for large antenna sizes.

REFERENCES

1. Curzi, Giacomo, Dario Modenini, and Paolo Tortora. "Large constellations of small satellites: A survey of near future challenges and missions." *Aerospace* 7.9 (2020): 133.
2. Demirev, V. SCP-RPSC Technology in the Feeder Lines of the LEO, s Communication Systems. *Proceedings of CEMA*, *7*, 1-5.
3. Lu, Y., & Zheng, X. (2020). 6G: A survey on technologies, scenarios, challenges, and the related issues. *Journal of Industrial Information Integration*, 100158.
4. Lin, M., Lin, Z., Zhu, W. P., & Wang, J. B. (2018). Joint beamforming for secure communication in cognitive satellite terrestrial networks. *IEEE Journal on Selected Areas in Communications*, *36*(5), 1017-1029.
5. Li, F., Lam, K. Y., Zhao, N., Liu, X., Zhao, K., & Wang, L. (2018). Spectrum trading for satellite communication systems with dynamic bargaining. *IEEE Transactions on Communications*, *66*(10), 4680-4693.
6. Hui, H., Ding, Y., Shi, Q., Li, F., Song, Y., & Yan, J. (2020). 5G network-based Internet of Things for demand response in smart grid: A survey on application potential. *Applied Energy*, *257*, 113972.
7. Metcalfe, K., Bréheret, N., Chauvet, E., Collins, T., Curran, B. K., Parnell, R. J., ... & Godley, B. J. (2018). Using satellite AIS to improve our understanding of shipping and fill gaps in ocean observation data to support marine spatial planning. *Journal of Applied Ecology*, *55*(4), 1834-1845.
8. Claudet, J., Bopp, L., Cheung, W. W., Devillers, R., Escobar-Briones, E., Haugan, P., ... & Gaill, F. (2020). A roadmap for using the UN Decade of ocean science for sustainable development in support of science, policy, and action. *One Earth*, *2*(1), 34-42.
9. Burleigh, Scott C., et al. "From connectivity to advanced Internet services: A comprehensive review of small satellites communications and networks." *Wireless Communications and Mobile Computing* 2019 (2019).
10. Li, B., Fei, Z., & Zhang, Y. (2018). UAV communications for 5G and beyond: Recent advances and future trends. *IEEE Internet of Things Journal*, *6*(2), 2241-2263.
11. De Gaudenzi, R., Angeletti, P., Petrolati, D., & Re, E. (2020). Future technologies for very

high throughput satellite systems. *International Journal of Satellite Communications and Networking*, *38*(2), 141-161.

12. Saeed, N., Almorad, H., Dahrouj, H., Al-Naffouri, T. Y., Shamma, J. S., & Alouini, M. S. (2020). Point-to-Point Communication in Integrated Satellite-Aerial Networks: State-of-the-art and Future Challenges. *arXiv preprint arXiv:2012.06182*.
13. Mehedi, S. A. H. M. M., Hasan, A. M., Sadiq, M. A., Akhtar, H., & Islam, L. S. R. (2020). A systematic review on practical considerations, recent advances and research challenges in underwater optical wireless communication.
14. Pokorny, J., Ometov, A., Pascual, P., Baquero, C., Masek, P., Pyattaev, A., ... & Koucheryavy, Y. (2018). Concept design and performance evaluation of UAV-based backhaul link with antenna steering. *Journal of Communications and Networks*, *20*(5), 473-483.
15. Qonita, A. H., & Muhtadin, N. (2019, May). Design and analysis of multibeam communication satellite links operated at Ka Band Frequency in Indonesia. In *IOP Conference Series: Earth and Environmental Science* (Vol. 284, No. 1, p. 012049). IOP Publishing.
16. Saeed, N., Al-Naffouri, T. Y., & Alouini, M. S. (2020). Wireless Communication for Flying Cars.
17. Gundamraj, A., Thatavarthi, R., Carter, C., Lightsey, E. G., Koenig, A., & D'Amico, S. (2021). Preliminary Design of a Distributed Telescope CubeSat Formation for Coronal Observations. In *AIAA Scitech 2021 Forum* (p. 0422).
18. Kumari, G., & Selwal, C. (2018). Performance Improvement in Inter-satellite Optical Wireless Communication to Mitigate Losses Using Diversity Technique. In *Optical and Wireless Technologies* (pp. 375-382). Springer, Singapore.
19. Babuscia, A., & Angkasa, K. (2020). Telemetry, tracking, and command (TT&C). In *Cubesat Handbook* (pp. 221-235). Academic Press.
20. Capela, C. J. R. (2012). Protocol of communications for VORSat satellite.
21. Brooker, R., & Vorderbrueggen, D. (2005, October). Antenna pointing accuracy impact on geostationary satellite link quality and interference. In *Proceedings of the 23rd AIAA International Communications Satellite Systems and 11th Ka and Broadband Communications Joint Conference, Rome, Italy*.
22. Bahadori, N., Namvar, N., Kelleyy, B., & Homaifar, A. (2019, April). Device-to-Device Communications in Millimeter Wave Band: Impact of Beam Alignment Error. In *2019 Wireless Telecommunications Symposium (WTS)* (pp. 1-6). IEEE.
23. Urata, K. N., Sri Sumantyo, J. T., Santosa, C. E., & Viscor, T. (2018). Development of an L-Band SAR Microsatellite Antenna for Earth Observation. *Aerospace*, *5*(4), 128.
24. Geudtner, D., Zink, M., Gierull, C., & Shaffer, S. (2002). Interferometric alignment of the X-SAR antenna system on the space shuttle radar topography mission. *IEEE Transactions on Geoscience and Remote sensing*, *40*(5), 995-1006.